PAPER

Rapid preparation of PAM/N-CNT nanocomposite hydrogels by DEM frontal polymerization and its performance study

Bin Li, [ID] *[a] Jizhen Liu, [ID] [a] Dandan Fu,[a] Yongjing Li,[b] Xiaojia Xu[a] and Ming Cheng [ID] [a]

In this study, a simple and eco-friendly method was proposed to efficiently prepare nanocomposite hydrogels with excellent mechanical properties and satisfactory pH response behaviour by frontal polymerization (FP) of DEM in close to 4 minutes. Acrylamide (AM) and choline chloride (ChCl) were used as raw materials to synthesize deep eutectic monomers (DEMs). Nitrogen-doped carbon nanotubes were dispersed in DEMs as fillers, and poly(acrylamide)/nitrogen-doped carbon nanotube (PAM/N-CNT) nanocomposite hydrogels were prepared by FP. The non-covalent interactions between PAM hydrogels and N-CNTs was verified by Fourier infrared spectroscopy. The mechanical properties of PAM/N-CNT nanocomposite hydrogels were investigated, as well as the swelling and pH response properties. The results showed that the compressive strength of PAM hydrogels was significantly enhanced by the addition of N-CNTs due to the hydrophobic interaction of N-CNTs, which also causes sensitive response properties of the PAM hydrogels in acid solution.

1. Introduction

Hydrogels are a 3D network configuration with polymer chains.[1] When exposed to specific external stimuli, such as water, they will absorb large amounts of water and then swell; the environmental factors like temperature, solvent quality, pH value and electric field can also cause the hydrogel to exhibit different properties, which promotes the wide range of application of hydrogels in various fields.[2–5] However, traditional single-component hydrogels have limited their applications in flexible wearable electronic devices,[6] drug transportation,[7] and environmental protection[8] due to their poor mechanical properties.

Carbon nanotubes are a kind of ideal polymer-reinforced nano-filler with large specific surface area. It is found that the mechanical properties of the polymer were significantly enhanced by adding a small amount of CNTs to the polymer matrix.[9] However, when CNTs are poorly compatible with the polymer matrix, it is difficult to disperse CNTs uniformly in the polymer matrix, which can directly affect the fracture toughness and tensile properties of the matrix.[10] There are many strategies to assist the dispersion of CNTs, such as: direct mixing,[10,11] chemical surface modification of CNTs,[12–14] *etc.* However, the above methods require complex modification work of CNTs or hybrid substrates in advance. Nitrogen-doped carbon

nanotubes, on the other hand, are designed to significantly enhance the dispersion properties by replacing the carbon atoms on the carbon hexameric ring backbone with nitrogen atoms, which in turn functionalizes the surface of CNTs.[15]

There are many polymerization methods for hydrogels, such as *in situ* polymerization,[16] suspension polymerization,[17] *etc.* These polymerization methods have disadvantages such as time consuming, energy consumption and low conversion rate. In contrast, frontal polymerization, as a new polymerization method, is able to rapidly converts monomers into polymers by reaction heat propagation. Compared with conventional polymerization, the self-propagating property of FP provides high conversion rate in a short time, greatly shortens the reaction time and saves the reaction cost.[18–20] FP has the ability to synthesize many polymer hydrogels, such as: *N*-isopropylacrylamide,[21] poly (acrylic acid-acrylamide)/activated carbon,[22] and poly (*N*-isopropylacrylamide-acrylic acid).[23] However, the difficulty in controlling the front velocity and front temperature limits its practical application.[24–26] Moreover, when water is used as the solvent, the violent reaction is accompanied by a large number of air bubbles that tend to lead to uneven product texture. In order to make the reaction smooth, bubble-free and continuous, the solvents used in FP are generally high-boiling organic solvents, such as dimethylformamide (DMF), dimethyl sulfoxide (DMSO), *etc.* In the production process, such toxic organic solvents can be hazardous to health and cause serious environmental pollution if not handled properly.[27]

Deep eutectic monomers (DEM) are binary mixtures of hydrogen-bond acceptor (HBA) and nonionic hydrogen bond donors (HBD).[28] As a new type of ILs with ionic liquid properties

[a]School of Mechanical Engineering, Wuhan Polytechnic University, Wuhan, Hubei 430023, China. E-mail: lb420@whpu.edu.cn

[b]Hubei Key Laboratory of Theory and Application of Advanced Materials Mechanics, Wuhan University of Technology, Wuhan, Hubei 430070, China

that are non-toxic and biodegradable. Components (different molar ratios mixed into different pairs of compounds). At present, there are numerous studies on the synthesis of polymers using DEM with frontal polymerization. Based on previous studies,[29] we investigated the effect of N-CNTs content on the behavior of FP by adding N-CNTs with better dispersion performance to DEM, and explored the effect of N-CNTs content on the mechanical properties and pH responsiveness of composite hydrogels, the polymerizable DEM solvent was prepared by heating the mixture of AM and ChCl in the molar ratio of 1 : 1. We found that the N-CNTs could be dispersed in the DEM uniformly, and the prepared hydrogels (Fig. 1) had excellent mechanical properties and pH responsiveness. We further analyzed the effect of N-CNTs content on FP, and investigated the effect of different N-CNTs content on the mechanical properties and pH responsiveness of the composite hydrogels.

2. Experimental

2.1. Materials

Nitrogen-doped carbon nanotubes (N-CNTs) were purchased from Hangzhou Hangdan Photoelectric Technology Company, with diameters of $30 \sim 50$ nm, lengths of $10 \sim 30$ μm, and 3% nitrogen content; acrylamide (AM) was purchased from Shanghai Aladdin Biochemical Technology Co. Ltd; choline chloride (ChCl) was dried at 80 °C to remove humidity before use; all reagents were of analytical grade and used directly; the water used in this experiment was ultrapure water.

2.2. Preparation of DEM

ChCl was chosen as HBA and AM as HBD. The two ingredients were physically stirred in a molar ratio of 1 : 2 in an oil bath at 70 °C until a homogeneous clear liquid, *i.e.* DEM, was obtained. The prepared DES was left to stand at 25 °C for a period of time, and the N-CNTs were added to the DEM according to the ratio in Table 1 and stirred until homogeneous.

2.3. Preparation of hydrogels by frontal polymerizations

The initiator KPS and crosslinker MBA were mixing with the mixture of DEM and N-CNTs. After a rest time of 60 s in a test tube, it was transferred to a long tube reactor (10 mm diameter and 100 mm long), and then treated with vacuum to eliminate

Table 1 Feed composition of samples during FP

Samples	AM/ChCl (molar ratio)	N-CNTs (wt%)	MBA (wt%)	KPS (wt%)
FP0	2 : 1	0	1	0.5
FP1	2 : 1	0.2	1	0.5
FP2	2 : 1	0.5	1	0.5
FP3	2 : 1	1.0	1	0.5

the air bubbles generated during stirring. A 200 °C soldering iron was placed against the upper face of the solution for thermal initiation, and the upper end of the reactor was kept under atmospheric pressure, and the iron was removed when a reaction front appeared. After the reaction, the prepared sample was removed from the test tube, cut into small pieces and soaked in deionized water for one week to dissolve the dissolvable material. The obtained nanocomposite hydrogels were freeze–dried to constant weight and stored for further testing.

2.4. Front velocity and temperature measurements

Frontal polymerization reactions generally have a constant front-end movement velocity (V_f), which can be determined by measuring the front-end position change *versus* time. To monitor the front-end temperature (T_{max}) change, the temperature of the front position was measured at room temperature by clamping the gripper at 10 mm from the top of the tube and immersing a K-type thermocouple connected to a digital thermometer in the liquid and placing it 70 mm from the liquid surface.

2.5. Material characterization and performance testing

The solid specimens were made into powder and mixed with potassium bromide, ground, pressed and tested by FTIR using a Nicolet 6700 FTIR spectrometer. The freeze–dried specimens were taken, and their cross-sections were sprayed with gold using a high-vacuum ion sputterer, and their cross-sectional microscopic morphology was observed by a MIRA 3 field emission scanning electron microscope (SEM).

The swelling properties of the prepared hydrogels were measured by weight analysis. A portion of the dry gel was soaked in deionized water and kept at 25 °C throughout to reach equilibrium. The soaked hydrogels were then removed at intervals and weighed after absorbing the surface water with filter paper until the swelling equilibrium was reached. The swelling rate SR was calculated using the following equation:

$$SR = (W_t - W_0)/W_0 \qquad (1)$$

where W_t denotes the weight of the dissolved hydrogel at time t and W_0 is the weight of the dry gel.

The hydrogel was tested by compression experiments using a Shanghai Baosheng TA.XTC-18 type mass spectrometer. Before the test, the hydrogel was soaked and cut into small cylinders of 10 mm in diameter and 10 mm in length. The compression experiments were carried out at a speed of 3
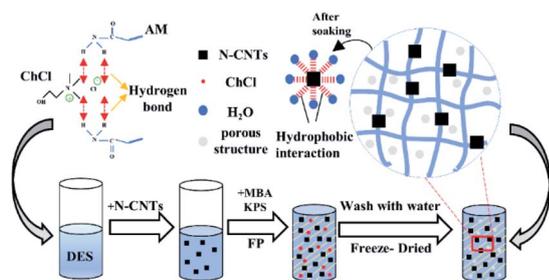

Fig. 1 Schematic diagram of the preparation of nanocomposite hydrogel.

mm min^{-1} until the maximum compressive stress was obtained. The material compressive strength P was calculated as follows:

$$P = F/S \tag{2}$$

where F is the applied force and S is the surface area of the hydrogel.

Fig. 3 (a) Front position-time curves of FP; (b) front temperature profiles of FP.

3 Results and discussion

3.1. Preparation of nanocomposite hydrogels by FP

Nanocomposite PAM/N-CNTs hydrogels were prepared by mixing N-CNTs with DEM using FP. N-CNTs and DEM were mixed together with strong stirring to obtain a highly dispersed homogeneous black mixture as shown in Fig. 2. The stirred DEM (with or without N-CNTs) was transferred to the long test tube used for FP, and then mixing with initiator KPS under the action of the initiator, the exothermic property of acrylamide promoted the temperature of the adjacent part of the test tube to rise dramatically, which in turn triggered the polymerization of the dispersed monomers. Meanwhile, the polymerized monomers raised the temperature of the liquid that promoted the polymerization reaction, which cyclically influenced and promoted each other. Finally, the temperature frontier at the temperature front would develop along the test tube at a constant rate, the processes of FP was completed in close to 4 minutes.

The temperature and velocity of the propagation front were measured by a K-type thermocouple, which was inserted 70 mm below the solution level. Constant velocity is one of the important characteristics of FP.[30,31] The front position *versus* time for different N-CNTs content is shown in Fig. 3a. It is illustrated that the front position is linear with respect to time, indicating that the front velocity is a constant and that this is pure FP with no spontaneous polymerization generated.[32,33]

The relationship between the content of N-CNTs on the front-end temperature *versus* time is shown in Fig. 3b. The front velocity (V_f) is found to increases from 20 cm min^{-1} to 28.6 cm min^{-1} when the N-CNTs content increases from 0.1 wt% to 1.0 wt%. With the increase of N-CNTs content. The isothermal region and the temperature extreme point (the maximum temperature of the front–end) can also be observed in the figure. The front temperature (T_{max}) also increased from 156.8 °C to 164.2 °C. This can be attributed to the fact that N-CNTs increases the liquid viscosity of the DEM as an
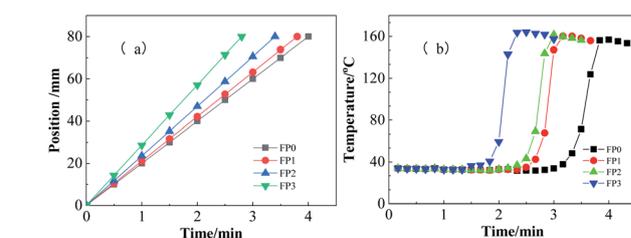
additional cross-linker, which leads to a higher front temperature. As a result, the polymerization rate (V_f) was faster and the front-end temperature (T_{max}) was higher after the addition of N-CNTs.

3.2. Characterization

The chemical structure of hydrogels was also characterized by FTIR. Fig. 4 shows the FTIR spectra of N-CNTs, PAM and PAM/N-CNTs.

From Fig. 4a, it can be seen that the PAM without filler addition has a strong absorption peak at 3430 m^{-1}, which is formed due to the NH stretching vibration. The absorption peak at 1656 m^{-1} is attributed to the stretching vibration band generated by the C=O group on the amide group. While the absorption peak at 2936 m^{-1} is the C–H band of asymmetric vibration, which is formed due to the C=C cleavage during the polymerization of acrylamide.[34] Fig. 4b represents the FTIR spectra of pure N-CNTs. The intensity of the absorption peaks of the N-CNTs is very weak and shows no significant peaks compared to the other two hydrogel IR spectral profiles. This indicates that there are fewer meaningful functional groups in the pristine N-CNTs.[35,36] In the FTIR spectra curves of PAM/N-CNTs, the absorption peaks generated by NH stretching vibrations in PAM and the stretching vibration bands generated by C=O groups were consistent with the bands of absorption peaks generated by pure PAM, and no shift of the bands to high or low frequencies was found, but a small shoulder peak appeared at 3237 m^{-1} of the PAM/N-CNTs curve. The above phenomena suggest that intermolecular noncovalent interactions generated by electron transfer may have occurred in the PAM/N-CNTs hydrogel, which confirms the formation of complexation between PAM and N-CNTs.[37]
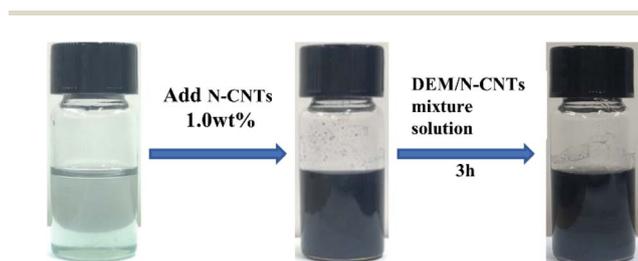

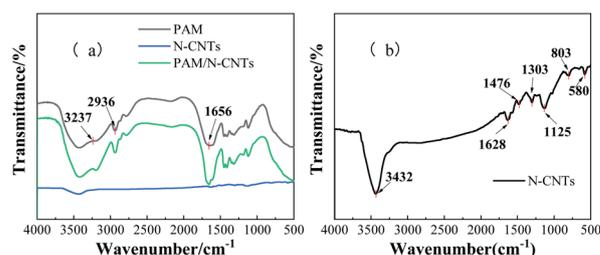Fig. 2 DEM/N-CNTs solutions (N-CNTs: 1.0 wt%).

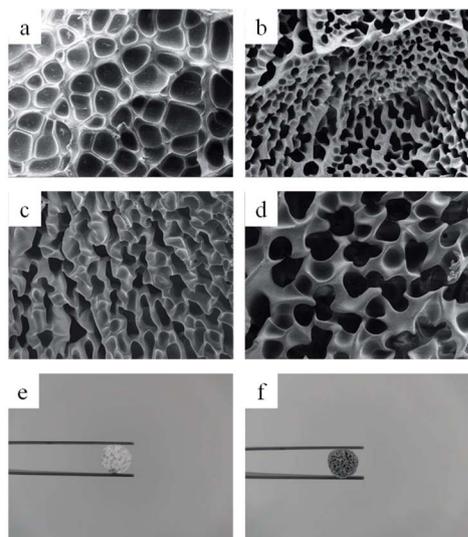Fig. 4 (a) FTIR of freeze-dried hydrogels (b) FTIR of N-CNTs.

Fig. 5 SEM images of freeze–dried (a) FP0, (b) FP1, (c) FP2, (d) FP3 hydrogels; photographs of freeze−dried FP0 (e), FP3 (f) hydrogels.

The cross-sectional morphology of the hydrogel are shown in Fig. 5. The effect of N-CNTs on the internal structure of PAM was investigated by observing the cross-sectional morphology of the composite hydrogels after washing by SEM. Before SEM, the pre-frozen dissolved target hydrogels were put into a freeze–dryer at -50 °C. At this time, the sublimation of the ice crystals filled in the pores of the hydrogel would result in the porous structure of hydrogels, as shown in Fig. 5. This is consistent with the results of previous work,[29] and the homogeneous porous structure indicates that the N-CNTs have been uniformly distributed and bound into the hydrogel. In addition, the PAM/N-CNTs hydrogel exhibited a homogeneous porous structure similar to that of pure PAM, except for the difference in porous densities. The porous size became smaller, while the densities increased with the addition of N-CNTs due to the effect of additional cross-linking agent produced by N-CNTs, while the addition of 1.0 wt% N-CNTs exhibited a slightly larger porous size. With the addition of N-CNTs, the mesh wall thickness of the hydrogel increased as shown in the figure. This may be due to the functionalization of carbon nanotubes, which resulted in N-CNTs with better dispersion properties and thus better compatibility with the polymer matrix.

3.3. Mechanical properties of nanocomposite hydrogels

Fig. 6 shows the stress-strain curves of the N-CNTs-doped hydrogel. The maximum compressive strength of PAM without filler doping is found to be 19.8 kPa, and the maximum compressive strength of 1.0% carbon nanotubes doping is 59.9 kPa. In the pure PAM compression experiments, the maximum compressive strength occurred at 25% of the deformation, and when the filler was doped, the maximum compressive strength all occurred at 35%. The results indicated that the addition of N-CNTs can both enhanced the compressive strength and stiffness of the hydrogel. Meanwhile, it is found that the hydrogels with N-CNTs addition exhibited larger elastic modulus, and the
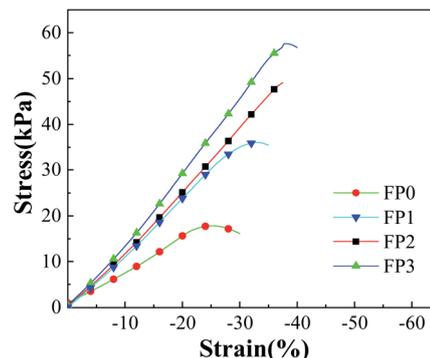

Fig. 6 The compressive stress-strain curve of nanocomposite hydrogel.

elastic modulus changed in the order of FP3 > FP2 > FP1 > FP0; the pure PAM compressive elastic modulus exhibited lower values and increased with the N-CNTs content. Awasthi[38] concluded that the mechanical properties of CNTs-polymer composites are highly dependent on the dispersion of CNTs, which directly affects the molecular tube–tube and tube-polymer interactions in the composites. This intermolecular interaction plays a key role in the load transfer and interfacial bonding, which determines the mechanical properties of the composites. This can be attributed to the presence of hydrophobic N-CNTs. The hydrophilic component are replaced by hydrophobic N-CNTs, resulting in a thinner wall-thick porous network structure.[39] The hydrophobic interaction between the N-CNTs and water molecules then enhances the intermolecular forces.[40] It also can be observed that the N-CNTs alignment effect has a greater role in obtaining different elastic moduli for hydrogel with low N-CNTs content. The stress–strain curves of all four hydrogels are linear under low stress, indicating that elastic deformation occurs under low stress conditions, which means that if the hydrogels are subjected to an applied load, the polymer chains are rearranged to accommodate the deformation. At the same time, a retraction elastic force was generated in the polymer network due to the tendency of the polymer network to recover its original conformation.[41]

3.4. Swelling behaviour at different pH values

The dissolution kinetic curves of hydrogels with different mass fractions of N-CNTs added are shown in Fig. 7. It can be seen from the figures that the equilibrium swelling of the hydrogels decrease with the N-CNTs content. Since the addition of N-CNTs promoted the physical entanglement of the long chains of macromolecules, which led to the increase of cross-link density and thus the decrease of the swelling properties of hydrogels. In addition, since PAM is a hydrophilic macromolecule, the equilibrium swelling of each group is kept at a high level.

PAM is a nonionic polymer, which cannot be ionized in water, but can be hydrolyzed in different pH solutions, so the adsorption of water molecules by the three-dimensional network of the polymer will give different results in different pH values. Fig. 8 show the swelling behavior of PAM hydrogels
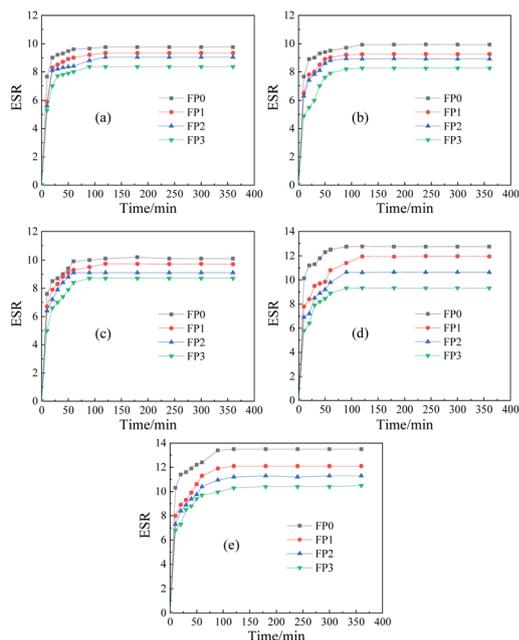
Fig. 7 Swelling kinetics curve (a) pH = 3; (b) pH = 4.8; (c) pH = 7; (d) pH = 9.4; (e) pH = 10.8.
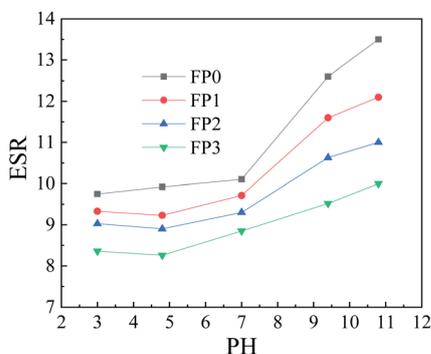

Fig. 8 Effect of nanocomposite hydrogels at various pH values.

and PAM/N-CNTs composite hydrogels at different pH values. As can be seen from the figure, the PAM/N-CNTs hydrogel samples maintained high equilibrium swelling in all pH ranges due to the fact that PAM is a hydrophilic macromolecule in which the amide group can form hydrogen bonds with water and is highly hydrophilic. For pure PAM, the PAM long chain solubility stays at a more stable level at pH < 7, while at pH > 7, the PAM solubility produces a large increase at a certain pH value. This is because under acidic conditions, $-CONH_2$ is not hydrolyzed and the polymer network is in a contracted state, so the change of pH value has little effect on the swelling performance, while under alkaline conditions, due to the hydrolysis of polyacrylamide side chain $-CONH_2$ into $-COOH$ or $-COO-$, the ionization of $-CONH_2$ increases the swelling permeation pressure, while the negatively charged $-COO-$ brings a negative charge to the network, and there is mutual repulsion between similar charges, these reasons lead to the swelling between the

long chains of the polymer, and the polymer swelling increases.[42,43] The introduction of carbon nanotubes after the introduction of carbon nanotubes (FP1, FP2, FP3 compared to FP0), the swelling properties of the hydrogels are reduced to some extent, probably due to the attachment of the bundled N-CNTs to the surface of the macromolecular chains through noncovalent interactions (as demonstrated in FTIR spectroscopy), which causes the oxygen-containing groups on the long polymer chains to be "swallowed", reducing the number of hydrophilic groups, while this noncovalent interactions may make the binding ability between PAM long chains and water molecules weaker, which in turn slows down the adsorption of water by polymer long molecular chains.[44,45]

4. Conclusions

The PAM/N-CNTs nanocomposite hydrogels were prepared by using FP to synthesize polymerizable DEM with AM and ChCl as raw materials and N-CNTs as fillers. The structure and properties of the composite gels were experimentally investigated, and the results showed that:

(1) Compared with the conventional preparation method, FP has a faster reaction and greener raw materials in the preparation of nanocomposite hydrogels. PAM/N-CNTs nanocomposite hydrogels were synthesized by FP, and with the increase of N-CNTs content, V_f increased from 20 to 28.6 cm min^{-1} and T_{max} increased from 156.8 to 164.2 °C. Due to the good dispersion of N-CNTs, the composite hydrogels showing a uniform porous structure were prepared, while N-CNTs were well compatible with the polymer matrix.

(2) The composite hydrogel has pH responsiveness, and the composite hydrogel containing N-CNTs shows better responsiveness in the acid solutions, which has certain application prospects in the slow release of drugs.

(3) Due to the hydrophobic effect of carbon nanotubes, the compressive strength and stiffness of the hydrogel increased with the increase of N-CNTs content. The compressive strength of the composite hydrogel containing N-CNTs 1% can reach up to 59.9 kPa, which was 3.03 times that of the pure PAM hydrogel. This improvement is expected to make up for the shortcomings of the hydrogel with limited application scope due to the lack of mechanical properties.

Author contributions

B. L., proposed the ideas, steps and details of the experiment, most of the experiments were done by J. Z. L., X. J. X, M. C., where J. Z. L., was instrumental in the proper conduct of the experiments and wrote the article together with B. L., and all the authors analyzed the data, discussed the conclusions.

Conflicts of interest

The authors declare that there are no competing interests regarding the publication of this article.

Acknowledgements

References

1 A. Marrella, A. Lagazzo, F. Barberis, T. Catelani, R. Quarto and S. Scaglione, *Carbon*, 2017, **115**, 608–616.

2 B. W. Walker, R. P. Lara, E. Mogadam, C. H. Yu, W. Kimball and N. Annabi, *Prog. Polym. Sci.*, 2019, **92**, 135–157.

3 H. Li, C. Tan and L. Li, *Mater. Des.*, 2018, **159**, 20–38.

4 Z. J. Shi, X. Gao, M. W. Ullah, S. X. Li, Q. Wang and G. Yang, *Biomaterials*, 2016, **111**, 40–54.

5 M. Shibayama and T. Tanaka, in *Responsive gels: volume transitions I*, Springer, 1993, pp. 1–62.

6 Y. Chen, S. Li and S. Yan, *Carbohydr. Polym.*, 2021, **263**, 117996.

7 X. Banquy, F. Suarez, A. Argaw, J.-M. Rabanel, P. Grutter, J.-F. Bouchard, P. Hildgen and S. Giasson, *Soft Matter*, 2009, **5**, 3984–3991.

8 P. M. Pakdel and S. J. Peighambardoust, *Carbohydr. Polym.*, 2018, **201**, 264–279.

9 G. A. Evingür and Ö. Pekcan, *Phase Transitions*, 2012, **85**, 553–564.

10 J. Sandler, M. Shaffer, T. Prasse, W. Bauhofer, K. Schulte and A. Windle, *Polymer*, 1999, **40**, 5967–5971.

11 J. Sandler, J. Kirk, I. Kinloch, M. Shaffer and A. Windle, *Polymer*, 2003, **44**, 5893–5899.

12 S. Banerjee, T. Hemraj-Benny and S. S. Wong, *Adv. Mater.*, 2005, **17**, 17–29.

13 K. Balasubramanian and M. Burghard, *small*, 2005, **1**, 180–192.

14 F. Mammeri, J. Teyssandier, C. Connan, E. Le Bourhis and M. M. Chehimi, *RSC Adv.*, 2012, **2**, 2462–2468.

15 L. Li, Y. Liu, X. Geng and B. An, *J. Phys. Chem.*, 2011, **27**, 443–448.

16 C. J. Landry, B. K. Coltrain, J. A. Wesson, N. Zumbulyadis and J. L. Lippert, *Polymer*, 1992, **33**, 1496–1506.

17 D. Maggioris, A. Goulas, A. Alexopoulos, E. Chatzi and C. Kiparissides, *Chem. Eng. Sci.*, 2000, **55**, 4611–4627.

18 N. Liu, H. Shao, C.-F. Wang, Q.-L. Chen and S. Chen, *Colloid Polym. Sci.*, 2013, **291**, 1871–1879.

19 I. D. Robertson, M. Yourdkhani, P. J. Centellas, J. E. Aw, D. G. Ivanoff, E. Goli, E. M. Lloyd, L. M. Dean, N. R. Sottos and P. H. Geubelle, *Nature*, 2018, **557**, 223–227.

20 S. Davtyan, A. Berlin and A. Tonoyan, *Rev. J. Chem.*, 2011, **1**, 56–92.

21 Q. Feng, F. Li, Q.-Z. Yan, Y.-C. Zhu and C.-C. Ge, *Colloid Polym. Sci.*, 2010, **288**, 915–921.

22 S. Li, H. Huang, M. Tao, X. Liu and T. Cheng, *J. Appl. Polym. Sci.*, 2013, **129**, 3737–3745.

23 Q. Feng, Q. Yan and C. Ge, *Colloid Polym. Sci.*, 2013, **291**, 1163–1170.

24 J. A. Pojman, *J. Am. Chem. Soc.*, 1991, **113**, 6284–6286.

25 I. P. Nagy, L. Sike and J. A. Pojman, *J. Am. Chem. Soc.*, 1995, **117**, 3611–3612.

26 J. A. Pojman, G. Curtis and V. M. Ilyashenko, *J. Am. Chem. Soc.*, 1996, **118**, 3783–3784.

27 S. Li and S. Yan, *RSC Adv.*, 2016, **6**, 33426–33432.

28 A. P. Abbott, G. Capper, D. L. Davies, R. K. Rasheed and V. Tambyrajah, *Chem. Commun.*, 2003, 70–71.

29 Y. Jiang, S. Li, Y. Chen, S. Yan, M. Tao and P. Wen, *Ind. Eng. Chem. Res.*, 2020, **59**, 1526–1533.

30 I. P. Nagy and J. A. Pojman, *J. Phys. Chem.*, 1996, **100**, 3299–3304.

31 S. Davtyan, A. Hambartsumyan, D. Davtyan, A. Tonoyan, S. Hayrapetyan, S. Bagyan and L. Manukyan, *Eur. Polym. J.*, 2002, **38**, 2423–2431.

32 T. Hu, Y. Fang, H. Yu, L. Chen and S. Chen, *Colloid Polym. Sci.*, 2007, **285**, 891–898.

33 J. A. Pojman, V. M. Ilyashenko and A. M. Khan, *J. Chem. Soc., Faraday Trans.*, 1996, **92**, 2825–2837.

34 J.-Z. Yi and L.-M. Zhang, *Eur. Polym. J.*, 2007, **43**, 3215–3221.

35 E. N. Konyushenko, J. Stejskal, M. Trchová, J. Hradil, J. Kovářová, J. Prokeš, M. Cieslar, J.-Y. Hwang, K.-H. Chen and I. Sapurina, *Polymer*, 2006, **47**, 5715–5723.

36 M.-L. Sham and J.-K. Kim, *Carbon*, 2006, **44**, 768–777.

37 Y. Luo, C. Wang and Z. Li, *Synth. Met.*, 2007, **157**, 390–400.

38 K. Awasthi, S. Awasthi, A. Srivastava, R. Kamalakaran, S. Talapatra, P. M. Ajayan and O. N. Srivastava, *Nanotechnology*, 2006, **17**, 5417–5422.

39 Y.-S. Chen, P.-C. Tsou, J.-M. Lo, H.-C. Tsai, Y.-Z. Wang and G.-H. Hsiue, *Biomaterials*, 2013, **34**, 7328–7334.

40 Z. Qin, X. Sun, Q. Yu, H. Zhang, X. Wu, M. Yao, W. Liu, F. Yao and J. Li, *ACS Appl. Mater. Interfaces*, 2020, **12**, 4944–4953.

41 F. A. Aouada, M. R. Guilherme, G. M. Campese, E. M. Girotto, A. F. Rubira and E. C. Muniz, *Polym. Test.*, 2006, **25**, 158–165.

42 B. Singh, G. S. Chauhan, S. Kumar and N. Chauhan, *Carbohydr. Polym.*, 2007, **67**, 190–200.

43 D. E. Rodríguez, J. Romero-García, E. Ramírez-Vargas, A. S. Ledezma-Pérez and E. Arías-Marín, *Mater. Lett.*, 2006, **60**, 1390–1393.

44 G. Akın Evingür and Ö. Pekcan, *Adv. Compos. Mater.*, 2012, **21**, 193–208.

45 G. A. Evingür and Ö. Pekcan, *J. Reinf. Plast. Compos.*, 2014, **33**, 1199–1206.